THE EUROPEAN PHYSICAL JOURNAL B

Regular Article

Spin-orbit interaction in the graphitic nanocone

Richard Pincak[1,2,a], Jan Smotlacha[2,3], and Michal Pudlak[1]

[1] Institute of Experimental Physics, Slovak Academy of Sciences, Watsonova 47, 043 53 Kosice, Slovak Republic
[2] Bogoliubov Laboratory of Theoretical Physics, Joint Institute for Nuclear Research, 141980 Dubna, Moscow region, Russia
[3] Faculty of Nuclear Sciences and Physical Engineering, Czech Technical University, Brehova 7, 110 00 Prague, Czech Republic

Abstract. The Hamiltonian for nanocones with curvature-induced spin-orbit coupling have been derived. The effect of curvature-induced spin-orbit coupling on the electronic properties of graphitic nanocones is considered. Energy spectra for different numbers of the pentagonal defects in the tip of the nanocones are calculated. It was shown that the spin-orbit interaction considerably affects the local density of states of the graphitic nanocone. This influence depends on the number of defects present at the tip of the nanocone. This property could be applied in atomic force microscopy for the construction of the probing tip.

1 Introduction

The spin-orbit interaction in graphene is supposed to be weak, due to the low atomic number of carbon. Spin-orbit coupling (SOC) in graphene has an intrinsic part, completely determined from the symmetry properties of the honeycomb lattice. The strength of this intrinsic spin-orbit coupling is rather small, due to weakness of the intra-atomic spin-orbit coupling of carbon. Because of the symmetry of the honeycomb lattice this intrinsic spin-orbit coupling vanishes for hopping between neighboring atoms [1]. To get the contribution from this kind of spin-orbit coupling we have to go to the next order in the hopping. In this paper we work with the tight-binding approximation where we take into account only the hopping between nearest neighboring atoms.

In a curved graphene sheet where the symmetry of honeycomb lattice is broken there is a possibility of curvature-induced spin-orbit coupling. A consistent approach to introduce this kind of SOC has been developed by Ando [2]. The experimental evidence for this kind of spin-orbit coupling was reported by Kuemmeth et al. [3]. It was demonstrated that in clean nanotubes the spin and orbital motion of electrons are coupled. In this work the authors measured the values of spin-orbit coupling in carbon nanotubes at various values of the magnetic field strength. It was revealed that the symmetry in electron-hole spectrum is broken. This can be caused by spin-orbit coupling.

In reference [4] the influence of SOC on the Kondo effect in carbon nanotube quantum dots was investigated by Fang et al. The results indicate that the spin-orbit coupling significantly changes the low-energy Kondo physics in carbon nanotube quantum dots. Recently,

Steele et al. [5] have reported the large spin-orbit coupling in carbon nanotubes. It turns out that the spin-orbit coupling could be significantly enlarged by the nonzero curvature of the nanoparticle surface [6–8]. Energy spectra and transport properties of armchair nanotubes with curvature-induced spin-orbit interactions were investigated by Pichugin et al. [9]. It was reported that due to spin-orbit coupling an armchair nanotube can serve in some energy range as an spin filter. To understand clearly quantum phenomena in carbon nanoparticles the spin-orbit coupling has to be included to describe their electronic properties. The spin-orbit coupling could also be important in nanocones due to their curved surface.

In this paper, we derive the effective Hamiltonian for the graphitic nanocone with spin-orbit coupling induced by curvature. The structure of the paper is as follows. In Section 2, we introduce an explicit formula for the eigenspectrum of the Hamiltonian with full curvature-induced spin-orbit coupling in a carbon nanocone. The solution is derived in the Appendices. In Section 3, we present numerical results for all of our calculations. The main conclusions are summarized in Section 4.

2 Dirac equation for curvature-induced spin-orbit coupling

The Hamiltonian has been derived following the method of Ando [2]. Adapting the derivation of Hamiltonian in reference [10], we introduce the curvature-induced spin-orbit interaction on the nanocone. We start with the Hamiltonian for the nanoconical surface without the spin-orbit coupling and pseudopotential [10,11]. Due to the rotational symmetry of the nanocone, we choose the radial and angular coordinates r, φ. Here, we will often use

[a] e-mail: pincak@saske.sk

$$\hat{H}' = \hbar v \begin{pmatrix} 0 & \partial_r - \mathrm{i}s\frac{1}{r(1-\eta)}\partial_\varphi - \frac{1}{2r} - \mathrm{i}\frac{1}{r}\xi_x\sigma_x - \frac{3}{2}\frac{\eta}{(1-\eta)r} - \frac{\xi_y\sigma_y}{r} \\ -\partial_r + \mathrm{i}s\frac{1}{r(1-\eta)}\partial_\varphi - \frac{1}{2r} + \mathrm{i}\frac{1}{r}\xi_x\sigma_x - \frac{3}{2}\frac{\eta}{(1-\eta)r} - \frac{\xi_y\sigma_y}{r} & 0 \end{pmatrix} \quad (5)$$
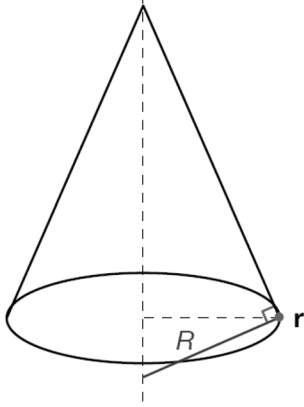

Fig. 1. The notation of the distances in the nanocone.

the coordinate R. It is the distance between the point $\mathbf{r}$ on the surface and the intersection of the conical axis with the line perpendicular to surface at point $\mathbf{r}$ (Fig. 1). It satisfies $R = \frac{(1-\eta)r}{\sqrt{\eta(2-\eta)}}$, where $\eta = N_d/6$ is the Frank index depending on N_d, the number of defects in the nanoconical tip.

The Hamiltonian has the form

$$\hat{H} = \begin{pmatrix} H_1 & 0 \\ 0 & H_{-1} \end{pmatrix}$$

$$H_s = \mathrm{i}\hbar v \left\{ \tau^y \partial_r - \tau^x r^{-1} \left[(1-\eta)^{-1} \left(s\partial_\varphi - \frac{3}{2}\mathrm{i}\eta \right) - \frac{1}{2}\tau^z \right] \right\}, \quad (1)$$

where τ^x, τ^y, τ^z are the Pauli matrices, $s = \pm 1$ denotes the value of the K spin.

Now, we will supply the terms corresponding to the spin-orbit interaction. It means that we perform the substitutions

$$\partial_r \rightarrow \partial_r - \frac{\delta\gamma'}{4\gamma}b_\varphi^\varphi\sigma_x(\mathbf{r}), \quad \mathrm{i}\partial_\varphi \rightarrow \mathrm{i}\partial_\varphi + s(1-\eta)A_y\sigma_y. \quad (2)$$

Here, $\sigma^x, \sigma^y, \sigma^z$ are the Pauli matrices corresponding to spin of electrons and we use the linear combination $\sigma_x(\mathbf{r}) = \sigma^x \cos\varphi - \sigma^z \sin\varphi$. The curvature of the surface is included in the curvature tensor $b_\varphi^\varphi = \frac{1}{R}$ and in the parameter $A_y = s\frac{2\delta p}{(1-\eta)}\sqrt{\eta(2-\eta)}$, which depends on the Frank index. The other parameters are described in reference [2] and they have the following meaning: the hopping integrals

$$\gamma = -\sqrt{3}V_{pp}^\pi a/2, \quad \gamma' = \sqrt{3}\left(V_{pp}^\sigma - V_{pp}^\pi\right)a/2,$$

where a is the length of the primitive translation vector ($a = \sqrt{3}d \simeq 2.46$ Å, d is the distance between atoms in the unit cell); V_{pp}^σ and V_{pp}^π are the transfer integrals

for the σ and π orbitals, respectively, in flat 2D graphite. Next, $p = 1 - 3\gamma'/8\gamma$, $\delta = \frac{1}{3}\frac{\Delta}{\epsilon_{\pi\sigma}}$, where

$$\Delta = i\frac{3\hbar}{4m^2c^2}\langle x|\frac{\partial V}{\partial x}p_y - \frac{\partial V}{\partial y}p_x|y\rangle \quad (3)$$

(V is the atomic potential) and $\epsilon_{\pi\sigma} = \epsilon_{2p}^\pi - \epsilon_{2p}^\sigma$. The energy ϵ_{2p}^σ is the energy of σ-orbitals that are localized between carbon atoms. The energy ϵ_{2p}^π is the energy of π-orbitals that are directed perpendicular to the nanotubular surface. The following values of the parameters are chosen: δ is of the order between 10^{-3} and 10^{-2}, $\frac{\gamma'}{\gamma} \sim \frac{8}{3}$, $p \sim 0.1$, $V_{pp}^\pi \approx -3$ eV and $V_{pp}^\sigma \approx 5$ eV, $p \approx 0.1$ and $\delta \approx 0.01$ [2]. Now, we will do the transformation

$$\hat{H}' = e^{\mathrm{i}\frac{\sigma_y}{2}\varphi}\hat{H}e^{-\mathrm{i}\frac{\sigma_y}{2}\varphi}. \quad (4)$$

With the aid of this transformation we describe the motion of an electron in the local coordinate frame which moves with the electron on the nanocone surface. Now we get:

see equation (5) above

where the parameters ξ_x, ξ_y describe the strength of the spin-orbit interaction:

$$\xi_x = \frac{\delta\gamma'\sqrt{\eta(2-\eta)}}{4(1-\eta)\gamma}, \quad \xi_y = A_y + \frac{1}{2(1-\eta)}. \quad (6)$$

Now, we are solving the equation

$$\hat{H}'\psi(r,\varphi) = E\psi(r,\varphi), \quad (7)$$

where, considering the rotational symmetry of the solution, we do the factorization

$$\psi(r,\varphi) = e^{\mathrm{i}j\varphi} \begin{pmatrix} f_{j\uparrow}(r) \\ f_{j\downarrow}(r) \\ g_{j\uparrow}(r) \\ g_{j\downarrow}(r) \end{pmatrix}. \quad (8)$$

Then, after the substitution of this expression into (7) and performing the differentiations with respect to φ, we have:

$$\begin{pmatrix} 0 & 0 & \partial_r + \frac{F}{r} & -\frac{\mathrm{i}}{r}C \\ 0 & 0 & -\frac{\mathrm{i}}{r}D & \partial_r + \frac{F}{r} \\ -\partial_r + \frac{F-1}{r} & \frac{\mathrm{i}}{r}D & 0 & 0 \\ \frac{\mathrm{i}}{r}C & -\partial_r + \frac{F-1}{r} & 0 & 0 \end{pmatrix} \begin{pmatrix} f_{j\uparrow}(r) \\ f_{j\downarrow}(r) \\ g_{j\uparrow}(r) \\ g_{j\downarrow}(r) \end{pmatrix}$$

$$= E \begin{pmatrix} f_{j\uparrow}(r) \\ f_{j\downarrow}(r) \\ g_{j\uparrow}(r) \\ g_{j\downarrow}(r) \end{pmatrix}, \quad (9)$$

where

$$F = \frac{sj}{1-\eta} - \frac{3}{2}\frac{\eta}{1-\eta} + \frac{1}{2}, \quad C = \xi_x - \xi_y, \quad D = \xi_x + \xi_y. \quad (10)$$

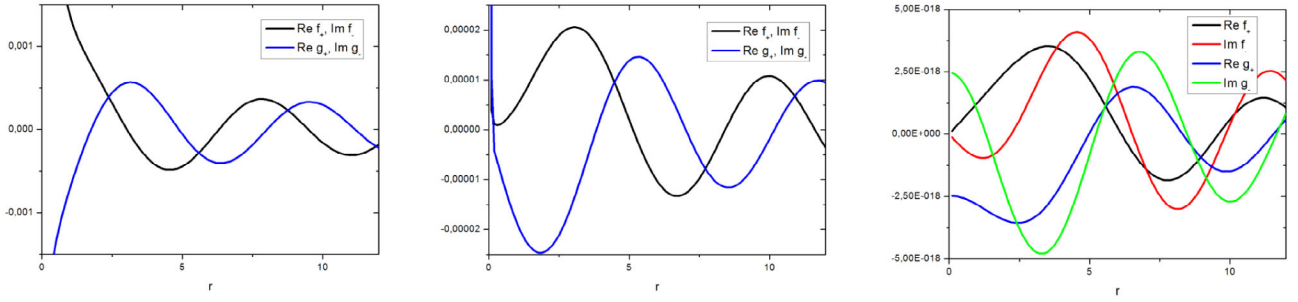The parameter $s = \pm 1$. The solution of (9) is given in Appendix A.

Fig. 2. Solution of the system (9) for the case of $N_d = 1$ (left), $N_d = 2$ (middle), $N_d = 3$ (right) and $E = 1$.
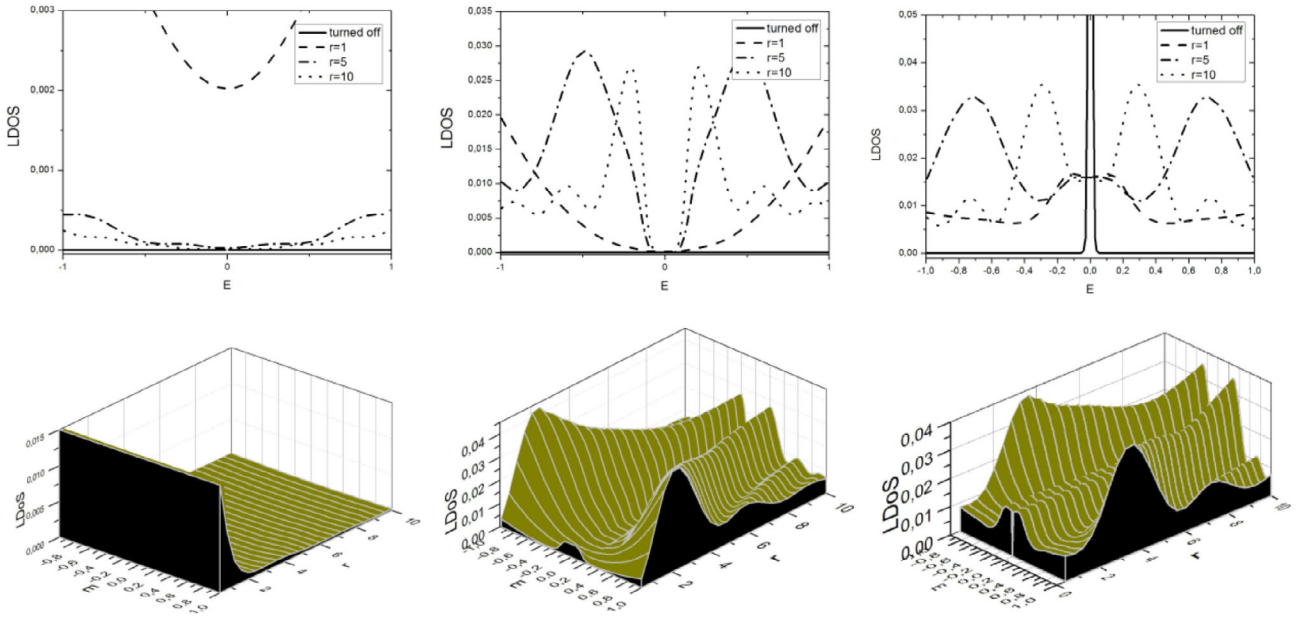

Fig. 3. 2D and 3D (bottom) graphs of the local density of states with and without (turned off) spin-orbital interaction for different distances r from the tip. $N_d = 1$ (left), $N_d = 2$ (middle) and $N_d = 3$ (right).

3 Electronic properties of the conical nanostructure

For $\beta = 1$ and $E = 1$, we see the solution of (9) in Figure 2. The signs $\uparrow, \downarrow$ in the indices are replaced here by the signs $+, -$, respectively. The graphs for Re $f_\downarrow$, Re $g_\downarrow$, Im $f_\uparrow$ and Im $g_\uparrow$ are missing – they provide the zero solution. We can see that for the cases of 1 and 2 defects, the modules of $f_\downarrow$, $f_\uparrow$ and $g_\downarrow$, $g_\uparrow$, respectively, coincide – the existing effect of the spin-orbit interaction is still not strong enough to split the appropriate components of the wave-function.

This solution has a form similar to Bessel functions of the first or the second kind (J_j or Y_j). This correspondence is derived in Appendix B for the case of $N_d = 1$ defect and $j = 2$. For other values of the energies or the parameter j, this occurrence will be similar.

For the normalized case, given energy and value of j, the local density of states ($LDoS$) is defined as:

$$LDoS(E,r) = |f_{j,E\uparrow}(r)|^2 + |f_{j,E\downarrow}(r)|^2$$
$$+ |g_{j,E\uparrow}(r)|^2 + |g_{j,E\downarrow}(r)|^2. \quad (11)$$

The numerical results are depicted in Figure 3. The solution without the spin-orbit interaction is the turned off case. For this case, the constants C and D would be equal to zero and the system (9) would be a 4-dimensional analogy of the 2-dimensional case without the spin-orbit interaction (described by Pincak et al. in Ref. [11]) and with the exclusion of the effect of the pseudopotential. This evidence can also be derived from the above plots in Figure 2, where the modules of the first and second or the third and fourth component, respectively, are not split unless the number of the defects in the conical tip exceeds 2.

4 Conclusion

An effective mass Hamiltonian was derived for a carbon nanocone in the presence of curvature-induced spin-orbit interaction. Within our approach, we solved analytically the eigenvalue problem for the effective mass Hamiltonian for electrons on the curved surface with the spin-orbit interaction. In particular, we obtained explicit expressions for a low-energy spectrum and eigenstates of carbon nanocones. The $LDoS$ in the graphitic nanocone

near the tip in the case of spin-orbit interactions were computed numerically. These findings have been used to analyze electronic properties of carbon nanocones with curvature-induced SOC at different limits. We see that the spin-orbit interaction considerably affects the local density of states of the graphic nanocone; the higher the number of defects, the bigger the effect. One of the reason is that the more defects present near the tip, the bigger the curvature of the nanocone in the vicinity of the tip, and so also the bigger the effect of the imposed spin-orbit interaction. The localization of the electrons as shown in Figure 3 makes the graphitic nanocone a possible candidate for the construction of a new type of scanning probe in atomic force microscopy [12–15].

Appendix A: Solution of the Dirac equation

We want to find the solution of (9) in the form

$$f_{j\uparrow}(r) = e^{\frac{\alpha}{r} + \beta r} \sum_{k=0}^{\infty} a_k r^{\xi+k},$$

$$f_{j\downarrow}(r) = e^{\frac{\alpha}{r} + \beta r} \sum_{k=0}^{\infty} b_k r^{\xi+k}, \qquad \text{(A.1)}$$

$$g_{j\uparrow}(r) = e^{\frac{\alpha}{r} + \beta r} \sum_{k=0}^{\infty} c_k r^{\xi_1+k},$$

$$g_{j\downarrow}(r) = e^{\frac{\alpha}{r} + \beta r} \sum_{k=0}^{\infty} d_k r^{\xi_1+k}. \qquad \text{(A.2)}$$

After the substitution, we get $\xi = \xi_1 - 2$ and

$$-\alpha c_0 = Ea_0, \quad -\alpha c_1 + \xi_1 c_0 + Fc_0 - iCd_0 = Ea_1,$$
$$-\alpha d_0 = Eb_0, \quad -\alpha d_1 + \xi_1 d_0 + Fd_0 - iDc_0 = Eb_1, \qquad \text{(A.3)}$$

$$\alpha a_0 = 0, \quad \alpha a_1 + \xi a_0 + (F-1)a_0 + iDb_0 = 0,$$
$$\alpha b_0 = 0, \quad \alpha b_1 - \xi b_0 + (F-1)b_0 + iCa_0 = 0, \quad \text{(A.4)}$$

$$\alpha a_2 - \beta a_0 + (F-\xi-2)a_1 + iDb_1 = 0,$$
$$\alpha b_2 - \beta b_0 + (F-\xi-2)b_1 + iCa_1 = 0, \quad \text{(A.5)}$$

$$\alpha a_3 - \beta a_1 + (F-\xi-3)a_2 + iDb_2 = 0,$$
$$\alpha b_3 - \beta b_1 + (F-\xi-3)b_2 + iCa_2 = 0. \quad \text{(A.6)}$$

For the other indices, we get the system of recurrence equations

$$-\alpha c_k + \beta c_{k-2} + (F + \xi_1 + k - 1)c_{k-1} - iCd_{k-1} = Ea_k,$$
$$-\alpha d_k + \beta d_{k-2} + (F + \xi_1 + k - 1)d_{k-1} - iDc_{k-1} = Eb_k, \qquad \text{(A.7)}$$

$$-\alpha a_k + \beta a_{k-2} - (F - \xi_1 + 2 - k)a_{k-1}$$
$$-iDb_{k-1} = -Ec_{k-4},$$
$$-\alpha b_k + \beta b_{k-2} - (F - \xi_1 + 2 - k)b_{k-1}$$
$$-iCa_{k-1} = -Ed_{k-4}. \quad \text{(A.8)}$$

If we suppose that $\alpha \neq 0$, we get the zero solution. So for the nontrivial solution $\alpha = 0$ and as follows from the first and the third equation in (A.3), in this case the coefficients a_0 and b_0 must be also zero. Then, from the system

$$(F - \xi_1)a_1 + iDb_1 = 0, \quad (F - \xi_1)b_1 + iCa_1 = 0 \quad \text{(A.9)}$$

follows:

$$\xi_1 = F \pm i\sqrt{CD}, \quad b_1 = \pm\sqrt{\frac{C}{D}}a_1. \qquad \text{(A.10)}$$

From the system

$$(F + \xi_1)c_0 - iCd_0 = Ea_1, \quad (F + \xi_1)d_0 - iDc_0 = Eb_1, \qquad \text{(A.11)}$$

we get

$$c_0 = \frac{(F + \xi_1)a_1 + iCb_1}{(F + \xi_1)^2 + CD}E, \quad d_0 = \frac{Eb_1 + iDc_0}{F + \xi_1}. \quad \text{(A.12)}$$

And from the system

$$(F - \xi_1 - 1)a_2 + iDb_2 = \beta a_1, \quad (F - \xi_1 - 1)b_2 + iCa_2 = \beta b_1, \qquad \text{(A.13)}$$

follows

$$b_2 = \beta\frac{(F - \xi_1 - 1)b_1 - iCa_1}{(F - \xi_1 - 1)^2 + CD}, \quad a_2 = \frac{\beta a_1 - iDb_2}{F - \xi_1 - 1}. \qquad \text{(A.14)}$$

Here, β is a free parameter. The following coefficients we get from the recurrence equations.

Now excluding the functions $f_{j\uparrow}, f_{j\downarrow}$ with the help of the first two equations in (9), we get a simplified system

$$-r^2 g''_{j\uparrow}(r) + (2F - 1)rg'_{j\uparrow}(r)$$
$$+ \left[F(F - 2) + D^2\right] g_{j\uparrow}(r) + ir(C + D)g'_{j\downarrow}(r)$$
$$- i(C - D)Fg_{j\downarrow}(r) = E^2 r^2 g_{j\uparrow}(r), \qquad \text{(A.15)}$$

$$ir(C + D)g'_{j\uparrow}(r) + i(CF - D)g_{j\uparrow}(r)$$
$$- ir(F - 1)Dg_{j\uparrow}(r) - r^2 g''_{j\downarrow}(r) - rg'_{j\downarrow}(r)$$
$$+ (C^2 + F^2)g_{j\downarrow}(r) = E^2 r^2 g_{j\downarrow}(r). \qquad \text{(A.16)}$$

To solve the problem an iteration method is used. For this purpose, we divide the components of the solution into the real and the imaginary part:

$$g_{j\uparrow} = \text{Re}\, g_{j\uparrow} + i\,\text{Im}\, g_{j\uparrow}, \quad g_{j\downarrow} = \text{Re}\, g_{j\downarrow} + i\,\text{Im}\, g_{j\downarrow}. \quad \text{(A.17)}$$

Now, for a given j, we denote

$$\mathrm{Re}\, g_{j\uparrow} = G_1, \quad \mathrm{Im}\, g_{j\downarrow} = G_2 \qquad (\mathrm{A.18})$$

and if we suppose that the conditions

$$\mathrm{Im}\, f_{j\uparrow} = \mathrm{Re}\, f_{j\downarrow} = \mathrm{Im}\, g_{j\uparrow} = \mathrm{Re}\, g_{j\downarrow} = 0 \qquad (\mathrm{A.19})$$

are satisfied for the analytical solution, for the nonzero components of $g_{j\uparrow}, g_{j\downarrow}$ we have:

$$-r^2 G_1''(r) + (2F-1)rG_1'(r) + \left[F(F-2)+D^2\right] G_1(r)$$
$$- r(C+D)G_2'(r) + (C-D)FG_2(r) = E^2 r^2 G_1(r), \qquad (\mathrm{A.20})$$

$$r(C+D)G_1'(r) + (CF-D)G_1(r) - r(F-1)DG_1(r)$$
$$- r^2 G_2''(r) - rG_2'(r) + (C^2+F^2)G_2(r) = E^2 r^2 G_2(r). \qquad (\mathrm{A.21})$$

This system can be rewritten into the form

$$r^2 G_1''(r) - (2F-1)rG_1'(r)$$
$$+ \left[E^2 r^2 - F(F-2) - D^2\right] G_1(r) = \mathfrak{D}_1(G_2(r)), \qquad (\mathrm{A.22})$$

$$r^2 G_2''(r) + rG_2'(r) + \left[E^2 r^2 - C^2 - F^2\right] G_2(r)$$
$$= \mathfrak{D}_2(G_1(r)), \qquad (\mathrm{A.23})$$

where $\mathfrak{D}_1, \mathfrak{D}_2$ on the right-hand side denote the differential operators. If we exclude them, we get the homogeneous parts of the system. For the second equation it gives the Bessel equation, for the first equation it gives a Bessel-like equation. It is not a problem to find a solution for this homogeneous system. We can try to find a particular solution for the inhomogeneous system in this way: let $G_{1-}^{(0)}, G_{1+}^{(0)}$ and $G_{2-}^{(0)}, G_{2+}^{(0)}$, respectively, denote the solution for the homogeneous system (actually, $G_{2-}^{(0)}, G_{2+}^{(0)}$ are the Bessel functions), then the particular solutions could be searched with the help of the method of variation of the constants, i.e. in the form

$$G_1(r) = C_{1-}(r)G_{1-}^{(0)}(r) + C_{1+}(r)G_{1+}^{(0)}(r),$$
$$G_2(r) = C_{2-}(r)G_{2-}^{(0)}(r) + C_{2+}(r)G_{2+}^{(0)}(r). \qquad (\mathrm{A.24})$$

Of course, there is the question of in which form the functions $G_1(r), G_2(r)$ would be substituted into the arguments of the operators $\mathfrak{D}_1, \mathfrak{D}_2$. In the first step, we could make a statement $C_{2-}(r) = C_{2+}(r) = 1$ and substitute $G_2(r)$ into the right-hand side of (A.22). In this way, we get the form of $C_{1-}(r), C_{1+}(r)$ and we can substitute $G_1(r)$ into the right-hand side of (A.23) acquiring more precise values of $C_{2-}(r), C_{2+}(r)$. This procedure can be repeated unless we achieve the required precision. We make a suggestion that the solution of (9) has a form of the Bessel-like functions. This estimate will be verified in the next section by comparison of the coefficients a_n, b_n, c_n, d_n with the coefficients corresponding to the Taylor series of the Bessel functions.
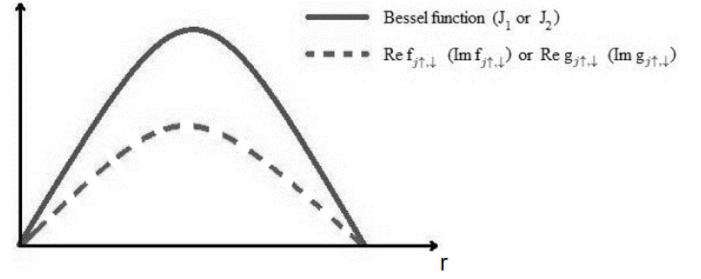

Fig. B.1. Comparison of the real or imaginary part of $f_{j\uparrow,\downarrow}$ ($g_{j\uparrow,\downarrow}$) and of the corresponding Bessel function. Here, the r coordinate denotes the distance from a tip. We have a boundary of a nanocone at $r_0 = 20$. We have zero probability of finding an electron at a boundary.

Table B.1. Correspondence of the Bessel function with solutions of (9) for $N_d = 1$ defect and different values of j.

j	$\mathrm{Re}\, f_{j\uparrow}$	$\mathrm{Im}\, f_{j\downarrow}$	$\mathrm{Re}\, g_{j\uparrow}$	$\mathrm{Im}\, g_{j\downarrow}$
0	$-Y_2$	$-Y_2$	Y_1	Y_1
1	$-Y_1$	$-Y_1$	J_1	J_1
2	J_1	J_1	J_2	J_2
3	J_2	J_2	J_3	J_3
4	J_3	J_3	J_4	J_4

Appendix B: Verification of the similarity between the solution and Bessel functions

Now we want to prove the correspondence between the solution of (9) and the Bessel functions. But first, we need to change the scale of the corresponding real or imaginary part of $f_{j\uparrow,\downarrow}$ or $g_{j\uparrow,\downarrow}$ such that the null points of the given function and the corresponding Bessel function correlate (see Fig. B.1). Then, we will do the described comparison for the case of 1 defect and $j = 2$ and the corresponding Bessel functions J_1 and J_2 (see Tab. B.1). The re-scaling we do numerically. For the value $E = 0.75$ and the unnormalized case, the re-scaled form of the solution of (9) has the form

$$f_{2\uparrow}^r(r) = e^{\frac{\alpha}{5.1103}r + \beta \frac{5.1103}{3.8317}r} \sum_{k=0}^{\infty} a_k \left(\frac{5.1103}{3.8317}r\right)^{\xi+k},$$

$$f_{2\downarrow}^r(r) = e^{\frac{\alpha}{5.1071}r + \beta \frac{5.1071}{3.8317}r} \sum_{k=0}^{\infty} b_k \left(\frac{5.1071}{3.8317}r\right)^{\xi+k}, \qquad (\mathrm{B.1})$$

$$g_{2\uparrow}^r(r) = e^{\frac{\alpha}{6.8490}r + \beta \frac{6.8490}{5.1356}r} \sum_{k=0}^{\infty} c_k \left(\frac{6.8490}{5.1356}r\right)^{\xi_1+k},$$

$$g_{2\downarrow}^r(r) = e^{\frac{\alpha}{6.8456}r + \beta \frac{6.8456}{5.1356}r} \sum_{k=0}^{\infty} d_k \left(\frac{6.8456}{5.1356}r\right)^{\xi_1+k}. \qquad (\mathrm{B.2})$$

We can do a shortcut of these expressions into the first 10 members of the expansion. Here, we choose $\alpha = 0$ and $\beta = 1$. Recalling that for the given values of

the parameters, $\xi_1 = 1.99987 \doteq 2$, we have:

$$\begin{aligned}
\operatorname{Re} f^r_{2\uparrow}(r) = f^r_{2\uparrow}(r) &\doteq 1.33r - 0.17r^3 + 6.95 \times 10^{-3}r^5 \\
&- 1.45 \times 10^{-4}r^7 + 1.81 \times 10^{-6}r^9 + \mathcal{O}(r^{10}),
\end{aligned} \tag{B.3}$$

$$\begin{aligned}
\operatorname{Im} f^r_{2\downarrow}(r) = f^r_{2\downarrow}(r) &\doteq -1.33182r + 0.17r^3 - 6.93 \times 10^{-3}r^5 \\
&+ 1.44 \times 10^{-4}r^7 - 1.80 \times 10^{-6}r^9 + \mathcal{O}(r^{10}),
\end{aligned} \tag{B.4}$$

$$\begin{aligned}
\operatorname{Re} g^r_{2\uparrow}(r) = g^r_{2\uparrow}(r) &\doteq 0.33r^2 - 2.78 \times 10^{-2}r^4 \\
&+ 8.69 \times 10^{-4}r^6 - 1.45 \times 10^{-5}r^8 \\
&+ 1.51 \times 10^{-7}r^{10} + \mathcal{O}(r^{11}),
\end{aligned} \tag{B.5}$$

$$\begin{aligned}
\operatorname{Im} g^r_{2\downarrow}(r) = g^r_{2\downarrow}(r) &\doteq -0.33r^2 + 2.77 \times 10^{-2}r^4 \\
&- 8.67 \times 10^{-4}r^6 + 1.45 \times 10^{-5}r^8 \\
&- 1.50 \times 10^{-7}r^10 + \mathcal{O}(r^{11}).
\end{aligned} \tag{B.6}$$

The corresponding expansions for the Bessel functions J_1, J_2 have the form

$$\begin{aligned}
J_1(r) &\doteq 0.5r - 0.06r^3 + 2.60 \times 10^{-3}r^5 - 5.43 \times 10^{-5}r^7 \\
&+ 6.78 \times 10^{-7}r^9 + \mathcal{O}(r^{10}),
\end{aligned} \tag{B.7}$$

$$\begin{aligned}
J_2(r) &\doteq 0.125r^2 - 0.01r^4 + 3.26 \times 10^{-4}r^6 - 5.43 \times 10^{-6}r^8 \\
&+ 5.65 \times 10^{-8}r^10 + \mathcal{O}(r^{11}).
\end{aligned} \tag{B.8}$$

Now, if we make a comparison of the coefficients corresponding to the power series of $\operatorname{Re} f^r_{2\uparrow}$, $\operatorname{Im} f^r_{2\downarrow}$, respectively, with the coefficients corresponding to J_1 and of the coefficients corresponding to the power series of $\operatorname{Re} g^r_{2\uparrow}$, $\operatorname{Im} g^r_{2\downarrow}$, respectively, with the coefficients corresponding to J_2, we find that more or less, for a concrete pair of functions, the ratio of the coefficients remains constant and it approaches these values:

$$\begin{aligned}
\frac{\operatorname{Re} f^r_{2\uparrow}(r)}{J_1(r)} &\doteq 2.67, & \frac{\operatorname{Im} f^r_{2\downarrow}(r)}{J_1(r)} &\doteq -2.66, \\
\frac{\operatorname{Re} g^r_{2\uparrow}(r)}{J_2(r)} &\doteq 2.67, & \frac{\operatorname{Im} g^r_{2\downarrow}(r)}{J_2(r)} &\doteq -2.66.
\end{aligned} \tag{B.9}$$

In Table B.1, we see the concrete forms of the Bessel functions which correspond to the case $N_d = 1$ defect and different values of the parameter j. However, the higher the value of j is, the more spread this correspondence is. On the whole, we can say that for the case of $N_d = 1$ defect and values of $j \geq 2$, the analytical expression for the solution can be approximated as:

$$\begin{aligned}
\operatorname{Re} f_{j\uparrow} &\sim J_{j-1}(Er), & \operatorname{Im} f_{j\downarrow} &\sim J_{j-1}(Er), \\
\operatorname{Re} g_{j\uparrow} &\sim J_j(Er), & \operatorname{Im} g_{j\downarrow} &\sim J_j(Er).
\end{aligned} \tag{B.10}$$

For the case of $N_d = 2$ and $N_d = 3$ defects, the corresponding tables would be more complicated, and the solution would be a linear combination of Bessel functions of different kinds.

References

1. C.L. Kane, E.J. Mele, Phys. Rev. Lett. **95**, 226801 (2005)
2. T. Ando, J. Phys. Soc. Jpn **69**, 1757 (2000)
3. F. Kuemmeth, S. Ilani, D.C. Ralph, P.L. McEuen, Nature **452**, 448 (2008)
4. T. Fang, W. Zuo, H. Luo, Phys. Rev. Lett. **101**, 246805 (2008)
5. G.A. Steele et al., Nat. Commun. **4**, 1573 (2012)
6. D. Huertas-Hernando, F. Guinea, A. Brataas, Phys. Rev. B **74**, 155426 (2006)
7. J.S. Jeong, J. Shin, H.W. Lee, Phys. Rev. B **84**, 195457 (2011)
8. M. del Valle, M. Marganska, M. Grifoni, Phys. Rev. B **84**, 165427 (2011)
9. K.N. Pichugin, M. Pudlak, R.G. Nazmitdinov, Eur. Phys. J. B **87**, 124 (2014)
10. Yu. A. Sitenko, N.D. Vlasii, Nucl. Phys. B **787**, 241 (2007)
11. R. Pincak, J. Smotlacha, M. Pudlak, Physica B **441**, 58 (2014)
12. I.-C. Chen et al., Appl. Phys. Lett. **88**, 153102 (2006)
13. J. Sripirom, S. Noor, U. Kohler, A. Schulte, Carbon **49**, 2402 (2011)
14. Ö. Karc, M. Dede, A. Oral, Rev. Sci. Instrum. **85**, 103705 (2014)
15. T. Nishio et al., Phys. Rev. B **77**, 012502 (2008)